OPTIMAL PLANE CHANGE DURING CONSTANT ALTITUDE HYPERSONIC FLIGHT

88-4341-CP

K. D. Mease*
Princeton University
Princeton, New Jersey

N. X. Vinh** and S. H. Kuo#
University of Michigan
Ann Arbor, Michigan

Abstract

In a previous paper, we addressed the problem of choosing constant values of altitude, speed, and angle of attack such that the plane change during hypersonic flight is maximized for a fixed amount of propellant consumption. In the present paper, the assumptions of constant speed and angle of attack are removed. Necessary conditions for solutions to the resulting optimal control problem are derived, and the general characteristics of the optimal controls are described using the domain of maneuverability. Numerical solutions are obtained for several specific cases. We find that, under the condition of constant altitude flight, it is not in general optimum to fly at constant angle of attack. The reduction in plane change capability resulting from a constant angle of attack program increases as the the range over which the flight takes place increases. On the other hand, the optimum speed is nearly constant.

Introduction

Future spacecraft operating in the vicinity of the Earth may use the atmosphere as an aid in changing orbits. The pioneering work of London[1] established that significant propellant savings are achievable, for certain orbital transfers, by employing a combination of aerodynamic force and propulsive force, rather than relying on propulsive force alone. One example of an "aeroassisted transfer" is the synergetic plane change, in which aerodynamic force is used in part to change the orbital plane of a spacecraft. Two possible flight modes for the atmospheric portion of a synergetic plane change are aeroglide and aerocruise. Aeroglide implies that there is no thrusting. Aerocruise implies that there is thrusting within the atmosphere. Moreover, steady aerocruise implies that the component of thrust along the velocity vector is adjusted to cancel drag and thereby hold the velocity constant and that the vertical components of thrust and lift are used to maintain constant altitude. The lateral components of lift and thrust change the orbital plane. A previous study[2] determined how the orbital plane changes during aerocruise and what values of the parameters, that define aerocruise, maximize the plane change. It was assumed that the angle of attack was constant, as were the altitude and velocity. Thus the optimization was of a parametric nature. While the consideration of constant angle of attack, constant velocity, constant altitude flight simplifies the mathematical analysis, there is no physical reason for insisting on this program. It may well be that larger plane changes for a given amount of propellant are possible, if these parameters are allowed to vary.

In the present paper, an intermediate case is considered, namely, constant altitude, variable velocity, and variable angle of attack flight. With this generalization, we are faced with a optimal control problem. The controls are taken to be the angle of attack, angle of bank, and thrust magnitude. The problem is to determine the control programs that maximize the plane change achieved for a given amount of propellant. Since the controls are bounded, the maximum principle is used to derive necessary conditions for the optimal controls. Based on the necessary conditions, a qualitative discussion of the types of optimal control solutions is given. In particular, the domain of maneuverability shows clearly the possible behaviors of the optimal bank angle. Numerical results are obtained for several specific cases.

Constant Altitude Optimal Control Problem

We shall consider the constant (high) altitude flight of a thrusting, lifting vehicle of mass m around the Earth. For the purpose of showing clearly the qualitative behavior of the optimal controls, a number of mathematically simplifying assumptions are made. The Earth is assumed to be nonrotating with a gravitational field and a stationary atmosphere that depend only on the radial distance from the center of the Earth. The trajectory variables ($r, \theta, \phi, V, \gamma, \psi$) are defined in Fig. 1, where r is the radial distance, θ is the longitude, ϕ is the latitude, V is the velocity magnitude, γ is the flight path angle relative to the local horizontal, and ψ is the heading angle relative to the local latitude line. We assume that the thrust is

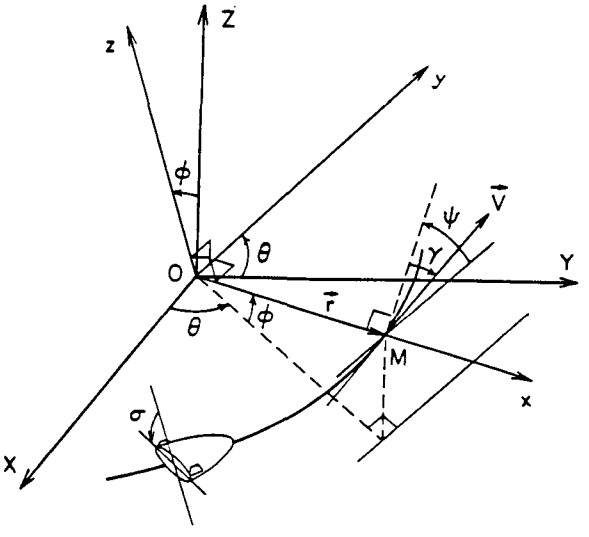

Fig. 1 State Variables and Bank Angle Defined with Respect to Inertial System OXYZ

---

* Assistant Professor, Mechanical and Aerospace Engineering, Senior Member AIAA

** Professor, Aerospace Engineering

\# Graduate Student, Aerospace Engineering, Present Address: Chung Shan Institute of Technology, Taiwan, Republic of China

aligned with the velocity vector **V**. Under these assumptions, the equations of motion for the vehicle are

$$\frac{dr}{dt} = V \sin\gamma$$

$$\frac{d\theta}{dt} = \frac{V \cos\gamma \cos\psi}{r \cos\phi}$$

$$\frac{d\phi}{dt} = \frac{V \cos\gamma \sin\psi}{r}$$

$$m\frac{dV}{dt} = T - D - mg\sin\gamma$$

$$mV\frac{d\gamma}{dt} = L\cos\sigma - mg\cos\gamma + \frac{mV^2}{r}\cos\gamma$$

$$mV\frac{d\psi}{dt} = \frac{L\sin\sigma}{\cos\gamma} - \frac{mV^2}{r}\cos\gamma\cos\psi\tan\phi$$

$$\frac{dm}{dt} = -\frac{T}{g\,I_{sp}} \qquad (1)$$

where T is the thrust, D is the drag force, L is the lift force, σ is the bank angle relative to local vertical plane (see Fig.1), I_{sp} is the specific impulse, and g is the gravitational acceleration. Consistent with the assumption of constant altitude flight, we have

$$r = R = \text{constant} \qquad \gamma = 0$$

In addition, the gravitational acceleration is assumed to be constant. The dimensionless arc length s will replace the time as the independent variable, where

$$s = \int_0^t \frac{V}{r}\,dt \qquad \Rightarrow \qquad \frac{ds}{dt} = \frac{V}{r} \qquad (2)$$

We shall assume a parabolic drag polar for the vehicle

$$C_D = C_{D0} + K C_L^2, \qquad (3)$$

where C_{D0} and K are assumed constant for hypersonic velocities. The following dimensionless variables are introduced

$$u = \frac{V^2}{gR}$$

$$\mu = \frac{m}{m_0} \qquad (4)$$

The variable u is a measure of the velocity magnitude. The variable μ is the ratio of the actual mass to the initial mass. Also, we define the dimensionless parameters and controls

$Z = \rho S R C_L^* / 2m_0$

$c = I_{sp}(g/R)^{1/2}$: dimensionless specific impulse

$\lambda = C_L / C_L^*$: normalized lift coefficient

$\tau = T / m_0 g$: dimensionless thrust (5)

Z is proportional to the density ρ and hence it is a parameter defining the flight altitude. C_L^* is the lift coefficient corresponding to the maximum lift-to-drag ratio. From the parabolic drag polar relation, we can calculate

$$C_L^* = \sqrt{C_{D0}/K}$$

$C_D^* = 2C_{D0}$: drag coefficient corresponding to the maximum lift-to-drag ratio

$$E^* = (C_L/C_D)_{max} = \frac{1}{2\sqrt{K C_{D0}}}$$

: maximum lift-to-drag ratio

Since $d\gamma/dt = 0$, we have the relation

$$\cos\sigma = \frac{(1-u)}{Z\lambda u}\mu \qquad (6)$$

which expresses that the vertical component of the lift force is used to balance the weight minus the centrifugal force. Thus, the lift coefficient, or equivalently, the angle of attack, and bank angle controls are not independent. Using Eq. (6), we eliminate λ in the equations of motion, leaving the choice of σ as the sole means of controlling the aerodynamic force.

By substituting the relations and parameters stated above into Eq. (1), we obtain the dimensionless state equations

$$\frac{d\theta}{ds} = \frac{\cos\psi}{\cos\phi}$$

$$\frac{d\phi}{ds} = \sin\psi$$

$$\frac{du}{ds} = \frac{2\tau}{\mu} - \frac{uZ}{E^*\mu}\left[1 + \frac{(1-u)^2\mu^2}{Z^2u^2\cos^2\sigma}\right]$$

$$\frac{d\psi}{ds} = \frac{(1-u)}{u}\tan\sigma - \cos\psi\tan\phi$$

$$\frac{d\mu}{ds} = -\frac{\tau}{c\sqrt{u}} \qquad (7)$$

The controls are the bank angle σ and the dimensionless thrust τ, subject to the inequality constraints

$$0 \le \tau \le \tau_{max} \qquad (8)$$

and

$$|\sigma| \le \cos^{-1}\left(\frac{(1-u)\mu}{Z\lambda_{max}u}\right) \qquad (9)$$

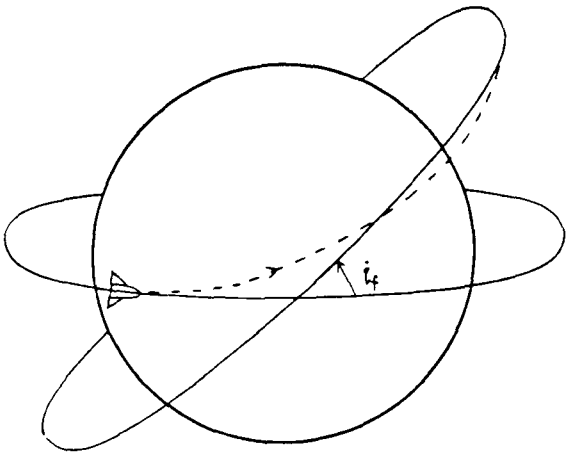

Fig. 2 The Inclination Angle i_f

At the initial time

$$s=0,\ \theta=0,\ \phi=0,\ \psi=0,\ \mu=1,\ u=u_0 \tag{10}$$

At the final time

$$s_f = \text{free},\ \theta_f = \text{free},\ \mu_f = \text{given},\ u_f = \text{given} \tag{11}$$

Since we want to maximize the inclination angle i_f (Fig. 2), we use the performance index

$$J = -\cos i_f = -\cos\phi_f \cos\psi_f \tag{12}$$

Analytic and Geometric Characterization of the Optimal Controls

Introducing the adjoint variables (P_θ, P_ϕ, P_u, P_ψ, P_μ), the Hamiltonian for the control problem is

$$H = P_\theta \frac{\cos\psi}{\cos\phi} + P_\phi \sin\psi - \frac{P_u u Z}{E^* \mu}\left[1 + \frac{(1-u)^2\mu^2}{Z^2 u^2 \cos^2\sigma}\right]$$
$$+ P_\psi\left[\frac{(1-u)}{u}\tan\sigma - \cos\psi\tan\phi\right] + \frac{2\tau}{\mu\sqrt{u}}\left[\sqrt{u}\,P_u - \frac{\mu P_\mu}{2c}\right] \tag{13}$$

Defining the switching function as

$$S = \sqrt{u}\,P_u - \frac{\mu P_\mu}{2c} \tag{14}$$

the Hamiltonian as a function of τ is maximized according to the rules:

	$S>0$,	$\tau=\tau_{max}$	(Boosting-arc)
If	$S=0$, then	τ=variable	(Sustaining-arc)
	$S<0$,	$\tau=0$	(Coasting-arc)

The adjoint variables satisfy the following differential equations

$$\frac{dP_\theta}{ds} = 0$$

$$\frac{dP_\phi}{ds} = -P_\theta \frac{\cos\psi}{\cos^2\phi}\sin\phi + P_\psi \frac{\cos\psi}{\cos^2\phi}$$

$$\frac{dP_\psi}{ds} = P_\theta \frac{\sin\psi}{\cos\phi} - P_\phi\cos\psi - P_\psi \sin\psi\tan\phi$$

$$\frac{dP_u}{ds} = \frac{P_u Z}{E^*\mu}\left[1 - \frac{(1-u^2)\mu^2}{Z^2 u^2\cos^2\sigma}\right] + \frac{P_\psi}{u^2}\tan\sigma - \frac{P_\mu \tau}{2c\,u^{3/2}}$$

$$\frac{dP_\mu}{ds} = -\frac{P_u u Z}{E^*\mu^2}\left[1 - \frac{(1-u)^2\mu^2}{Z^2 u^2\cos^2\sigma}\right] + \frac{2\tau P_u}{\mu^2} \tag{15}$$

Because of the fact that $dH/ds = \partial H/\partial s = 0$ and s_f is free, we have the Hamiltonian integral

$$H = C_0 = 0 \tag{16}$$

As a consequence of the assumed spherical symmetry, we have the integrals[3]

$$\begin{aligned} P_\theta &= C_1, \\ P_\phi &= C_2\sin\theta - C_3\cos\theta \\ P_\psi &= C_1\sin\phi + (C_2\cos\theta + C_3\sin\theta)\cos\phi \end{aligned} \tag{17}$$

From the end condition that θ_f is free, it follows that

$$C_1 = 0 \tag{18}$$

With respect to the bank angle, the Hamiltonian is maximized when $\sigma = \pm\sigma_{max}$ or at an interior point. The first order necessary condition for an interior maximum is

$$\frac{\partial H}{\partial \sigma} = 0$$

which leads to

$$\tan\sigma = \frac{E^* Z P_\psi}{2P_u(1-u)\mu} \tag{19}$$

This general formula is valid for all B-arcs, C-arcs and S-arcs. For H to be a maximum at a particular bank angle satisfying Eq. (19), we must have

$$\frac{\partial^2 H}{\partial\sigma^2} = -\frac{2P_u(1-u)^2\mu}{E^* Z u\cos^4\sigma} < 0 \tag{20}$$

This requires that $P_u > 0$.

It is enlightening to discuss the optimal bank angle control using the domain of maneuverability. For this purpose, we consider the reduced Hamiltonian containing the bank angle

$$\underline{H} = \frac{P_\psi(1-u)}{u}\tan\sigma - \frac{P_u(1-u)^2\mu}{E^* Z u}\times\frac{1}{\cos^2\sigma}$$

We write it in the form of the dot product of two vectors

$$\underline{H} = P_1 \Omega_1 + P_2 \Omega_2 = \mathbf{P} \cdot \Omega \tag{21}$$

where

$$P_1 = \frac{P_\psi (1-u)}{u} \qquad P_2 = -\frac{P_u (1-u)^2 \mu}{E^* Z u}$$

$$\Omega_1 = \tan\sigma \qquad \Omega_2 = \frac{1}{\cos^2\sigma} \tag{22}$$

The control domain described by the terminus of the vector Ω is a parabola with equation (Fig. 3)

$$\Omega_2 = 1 + \Omega_1^2 \tag{23}$$

At each instant, we consider the vector **P**. To maximize $\underline{H}$, the optimal vector Ω must be selected such that its projection onto **P** is maximized. If **P** is outside the angle $\Delta_1 O \Delta_2$, the optimal bank angle is $\sigma = \sigma_{max}$ or $\sigma = -\sigma_{max}$, according to whether $P_1 > 0$ or $P_1 < 0$. The rays $O\Delta_1$ and $O\Delta_2$ are respectively the perpendiculars to the tangents to the parabola at the points where $\sigma = -\sigma_{max}$ and $\sigma = \sigma_{max}$. If the vector **P** is inside the angle $\Delta_1 O \Delta_2$, the optimal bank angle is an interior bank, at the point where the tangent to the parabola is orthogonal to the vector **P**. The condition of orthogonality is

$$\frac{d\Omega_2}{d\Omega_1} = 2\Omega_1 = -\frac{P_1}{P_2} \tag{24}$$

Using the definitions (22), we obtain the optimal law (19). It is clear that a necessary condition for an interior optimum bank angle is that $P_2 < 0$, and hence $P_U > 0$. As a particular case, when $P_U > 0$ and $P_1 = 0$, that is $P_\psi = 0$, the bank angle passes through zero and reverses its direction. This will be the case frequently encountered in optimal constant altitude flight at very high altitude. Another interesting case of a bank reversal is the case where $P_U < 0$, that is $P_2 > 0$, and $P_\psi = 0$. In this case, the bank angle control is bang-bang; the bank angle changes from σ_{max} to $-\sigma_{max}$, or vice-versa. A singular case occurs, when $P_U < 0$ and $P_\psi = 0$ for a finite time interval. This is the case of chattering bank control where the bank angle switches rapidly between $-\sigma_{max}$ and σ_{max}. From the solution (17) for the adjoint P_ψ, we have

$$C_1 \sin\phi + (C_2 \cos\theta + C_3 \sin\theta)\cos\phi = 0 \tag{25}$$

Using Cartesian coordinates, with

$$\begin{aligned} x &= R\cos\phi\cos\theta \\ y &= R\cos\phi\sin\theta \\ z &= R\sin\phi \end{aligned} \tag{26}$$

we have

$$C_1 z + C_2 x + C_3 y = 0 \tag{27}$$

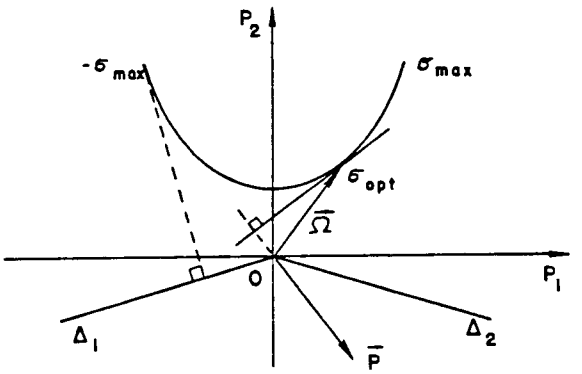

Fig. 3 Domain of Maneuverability for the Bank Angle

The chattering arc is a portion of a great circle, defined by the intersection of the plane defined by Eq. (27) and the sphere with radius R. The chattering arc is encountered in the case of minimum time deceleration control.

Assuming a C-arc or an S-arc, with the last term in the Hamiltonian vanishing, we can combine Eqs. (16)-(19) to obtain the following equation for the optimal bank angle along these arcs

$$AX^2 - 2BX + C = 0 \tag{28}$$

where

$$X = \frac{1-u}{u}\tan\sigma \tag{29}$$

and

$$\begin{aligned} A &= (k\cos\theta + \sin\theta)\cos\phi \\ B &= (k\cos\theta+\sin\theta)\cos\psi\sin\phi + (\cos\theta - k\sin\theta)\sin\psi \\ C &= -\frac{Z^2}{\mu^2}\left[1+\frac{(1-u)^2\mu^2}{Z^2u^2}\right](k\cos\theta+\sin\theta)\cos\phi \end{aligned} \tag{30}$$

where

$$k = C_2/C_3 \tag{31}$$

is a constant to be determined.

Along a sustaining-arc, which is a singular arc in the terminology of optimal control theory, we have, for a finite time interval,

$$P_u = \frac{\mu P_\mu}{2c\sqrt{u}} \tag{32}$$

By taking the derivative of this equation, using the state and adjoint equations, we have

$$\frac{P_\psi \tan\sigma}{u^2} = \frac{Z P_u}{2E^*\mu}\left\{\frac{(1-u)\mu^2}{Z^2u^2\cos^2\sigma}\left[(u+3)+(1-u)\frac{\sqrt{u}}{c}\right] - \left(1+\frac{\sqrt{u}}{c}\right)\right\} \tag{33}$$

Substituting Eq. (19) into Eq.(33), we obtain the optimal bank angle control for the sustaining-arc

$$\left(\frac{\sqrt{u}}{c} - 1\right) X^2 =$$

$$\frac{Z^2}{\mu^2}\left(\frac{\sqrt{u}}{c} + 1\right) - \frac{(1-u)}{u^2}\left[(u+3) + (1-u)\frac{\sqrt{u}}{c}\right] \quad (34)$$

There are always two solutions to Eq. (34): one positive and one negative. Going back to Eq. (19), because μ and adjoint P_u are positive for an interior optimal bank angle, it follows that X should always have the same sign as the adjoint P_ψ. Therefore, in numerical calculations, the sign of adjoint P_ψ should always be checked, at each time, to ensure that the vehicle is banking in the correct direction.

If we eliminate the bank control X between Eqs. (28) and (34), we have an equation relating the state variables along a sustaining arc

$$B^2\left(\frac{\sqrt{u}}{c} - 1\right)\left\{\frac{Z^2}{\mu^2}\left(\frac{\sqrt{u}}{c} + 1\right) - \frac{(1-u)}{u^2}\left[(u+3) + (1-u)\frac{\sqrt{u}}{c}\right]\right\}$$

$$= A^2\left\{\frac{Z^2}{\mu^2} - \frac{(1-u)}{u^2}\left[(1+u) + (1-u)\frac{\sqrt{u}}{c}\right]\right\}^2 \quad (35)$$

In the 5-dimensional state space ($\theta, \phi, \psi, u, \mu$), this equation represents a surface on which the sustaining arc lies. By taking the derivative of this equation and using the state equations (7) and the control law (34) for the bank angle, we obtain an equation for the variable thrust control

$$\tau = N / D \quad (36)$$

where

$$D = \frac{Z^2}{\mu^2}(\delta^2 - \delta - 1) + \frac{1}{u^2}\left[(1-u)^2\delta^3 + 3(1-u^2)\delta^2 + (1+3u^2)\delta - (3+u^2)\right] \quad (37)$$

$$N = -\frac{2uZ}{E^*}\left\{\frac{Z^2}{\mu^2} - \frac{1-u}{u^2}\left[(1+u) + (1-u)\delta\right]\right\}\left[\delta - \frac{\mu^2(1-u)}{Z^2u^2}(\delta+1)\right]$$

$$- \frac{uZ}{2E^*}\left[1 + \frac{\mu^2(1-u)^2}{Z^2u^2} + \frac{\mu^2}{Z^2}X^2\right]$$

$$\cdot \left\{\frac{Z^2}{\mu^2}(2-\delta) - \frac{2}{u^2}\left[(1-u^2)\delta^2 + (2u^2 - u + 1)\delta - (1+u^2)\right]\right\}$$

$$- \frac{uZ^2(\delta-1)^2}{2\mu(AX-B)}\left[A\sin\psi\tan\phi + (k\sin\theta - \cos\theta)\cos\psi\right]$$

$$\cdot X\left[1 + \frac{\mu^2(1-u)^2}{Z^2u^2} + \frac{\mu^2}{Z^2}X^2\right] \quad (38)$$

and

$$\delta = \frac{\sqrt{u}}{c} \quad (39)$$

In this expression $X = (1-u)\tan\sigma/u$ is computed from Eq. (34) and we see that the variable thrust is function of the state variables and the as yet unspecified constant $k=C_2/C_3$.

Application to Synergetic Plane Change

We are now ready to consider a synergetic plane change. In such an orbital transfer, the vehicle deorbits and enters the atmosphere at supercircular velocity. In order for the formulation and results presented above to be applicable, we consider the atmospheric trajectory to be composed of descent, constant altitude, and ascent segments. During the initial segment, the vehicle descends to the cruise altitude. During the constant altitude segment, the plane of the orbit is changed. At the end of the constant altitude segment, the vehicle is boosted to the desired orbital altitude. A circularization burn at orbital altitude completes the transfer. This form of a synergetic plane change, in which there is a constant altitude segment, corresponds to the case in which a heating rate inequality constraint limits the penetration into the atmosphere. More general treatments of the synergetic plane change[4,5] show that, when the unconstrained optimal trajectory violates the heating rate constraint, the constrained optimal trajectory has a finite segment along the constraint boundary, during which the altitude is approximately constant.

Previous results[2] have shown that the plane change is maximized, during constant altitude, constant velocity cruise, for a given amount of propellant, if the velocity is nearly circular. Thus, we expect that most of the optimal constant altitude segment will be a sustaining-arc. If the vehicle reaches the cruise altitude with supercircular velocity, the optimal trajectory will begin with a coasting-arc. If the velocity at the end of the sustaining-arc (when $\mu = \mu_f$) is less than the prescribed final velocity, the optimal trajectory will end with a boosting-arc.

These considerations lead us to consider initially the constant altitude segment as a pure sustaining-arc. Without any loss of generality, we can set the initial conditions to be

$$s_0 = 0, \quad \theta_0 = \phi_0 = \psi_0 = 0, \quad \mu_0 = 1 \quad (40)$$

from which it follows that

$$B_0 = 0 \quad (41)$$

Moreover, using the transversality condition at the final time, namely,

$$P_\phi(s_f) = \sin\phi_f \cos\psi_f \quad (42)$$

$$P_\psi(s_f) = \cos\phi_f \sin\psi_f \quad (43)$$

and Eqs. (17) and (18), we obtain

$$\frac{\sin\phi_f \cos\psi_f}{\cos\phi_f \sin\psi_f} = \frac{k \sin\theta_f - \cos\theta_f}{\cos\phi_f (k \cos\theta_f + \sin\theta_f)} \tag{44}$$

from which it follows that

$$B_f = 0 \tag{45}$$

So, at both ends, Eq. (28) gives the relation

$$X^2 = \frac{Z^2}{\mu^2} [1 + \frac{(1-u)^2 \mu^2}{Z^2 u^2}] \tag{46}$$

Substituting (46) into the equation for the optimal bank angle control, Eq. (34), gives the relation to be satisfied at the two ends of the sustaining-arc

$$\frac{Z^2}{\mu^2} = \frac{1-u}{u^2} [(1+u) + (1-u) \frac{\sqrt{u}}{c}] \tag{47}$$

By setting $\mu = 1$, we obtain a relation for computing the initial dimensionless velocity for the sustaining-arc

$$Z^2 = \frac{1-u_0}{u_0^2} [(1+u_0) + (1-u_0) \frac{\sqrt{u_0}}{c}] \tag{48}$$

Similarly, the equation for the final dimensionless velocity is

$$\frac{Z^2}{\mu_f^2} = \frac{1-u_f}{u_f^2} [(1+u_f) + (1-u_f) \frac{\sqrt{u_f}}{c}] \tag{49}$$

We see that u_0 and u_f are functions of the given parameters Z, c, and μ_f. Moreover, combining Eqs. (29), (41), (46), and (48) gives the initial bank angle for the sustaining-arc

$$\tan^2\sigma_0 = 1 + \frac{\sqrt{u_0}}{c} + \frac{1+u_0}{1-u_0} \tag{50}$$

Eq. (48) shows that for high altitude cruise, corresponding to small Z, u_0 is nearly unity; hence, the initial bank angle is nearly 90°.

Determining the optimum controls for the sustaining-arc, although the constant k is all that remains to be determined, requires numerical computation. We select a reference altitude by selecting a value of Z, an engine characteristic by seclecting a value of c, and the vehicle's aerodynamic characteristics by selecting a value of the maximum lift-to-drag ratio E^*. We choose

$$Z = 0.080640,\ c = 0.353612,\ E^* = 2.387 \tag{51}$$

which are the same values as used in Ref. 2. From the definition of Z (see Eq. 5), the value of Z selected corresponds to an altitude of about 75 km for a typical hypersonic vehicle, but it can be a higher altitude for a vehicle with lower wing loading $m_0 g/S$, or conversely, a lower altitude for a vehicle with higher wing loading. With these data, we compute the initial velocity for the constant altitude sustaining-arc from Eq. (48) and obtain $u_0 = 0.996779$. The integration of the state equations (7) can be performed using the initial condition (40). The bank angle control is given by Eq. (34); while, the thrust magnitude is given explicitly by Eq. (36). Furthermore, we can use Eq. (35) which is essentially the Hamiltonian integral along a sustaining-arc to check the accuracy of the numerical integration. It should be noted that to avoid numerical error in the evaluation of the bank angle, due to the behavior of the terms $(1-u)\tan\sigma$ and $(1-u)/\cos\sigma$ when $\sigma \approx 90^\circ$, we use the definition (29) to express these terms in terms of the control X, in the state equations (7) for the integration.

The optimum thrust control τ is known except for the arbitrary constant k. According to the necessary conditions, the constant k should be selected such that at the end of the sustaining-arc, where B=0, the prescribed final mass ratio μ_f is reached. However, this criterion can be satisfied by a countable infinity of k values; and the corresponding controls lead to either locally maximal or minimal values of the plane change. It remains to select the globally maximizing solution from the set of solutions that meet the necessary conditions. We examine this process, for the particular case under consideration, with the aid of Figs. 4-6.

For the selected altitude, two trajectories, corresponding to k=1.0 and k=0.5, are plotted in the u-μ plane in Fig. 4. (For positive k values, the vehicle begins turning in the leftward direction.) Note that the velocity oscillates as the mass decreases; but it is never far from circular velocity (u=1). The local minima in the velocity occur at the points where a trajectory touches the curve labelled "A=0". This curve has the following significance. Referring to Eq. 30, we see that A is equivalent to the adjoint P_ψ. Eq. (19) indicates that the bank angle is zero when P_ψ, or A, is zero. This occurs when the vehicle is near an apex of the osculating orbit and the bank angle is midway through a continuous, but quick, transition from $+90^\circ$ to -90° or vice-versa, i.e., midway through a bank reversal. For $\sigma = 0$, we have $X = 0$; and consequently, Eq. (34) reduces to a relation between the dimensionless velocity u and the mass ratio μ, at the bank reversal points, namely

$$\frac{Z^2}{\mu^2} (\frac{\sqrt{u}}{c} + 1) = \frac{1-u}{u^2} [(3 + u) + (1 - u) \frac{\sqrt{u}}{c}] \tag{52}$$

This relation gives rise to the curve labelled "A=0". Thus, intersections of this curve and a trajectory indicate the occurence of a bank reversal, as well as a local minimum in the velocity.

As stated above, the constant k is selected such that, when B=0, the prescribed final mass ratio is reached. We have also determined that B=0 at the beginning of a sustaining-arc. Combining Eqs. (34) and (28), we obtain

$$B (\frac{\sqrt{u}}{c} - 1) X = A \{ \frac{Z^2}{\mu^2} - \frac{1-u}{u^2} [(1+u) + (1 - u) \frac{\sqrt{u}}{c}] \} \tag{53}$$

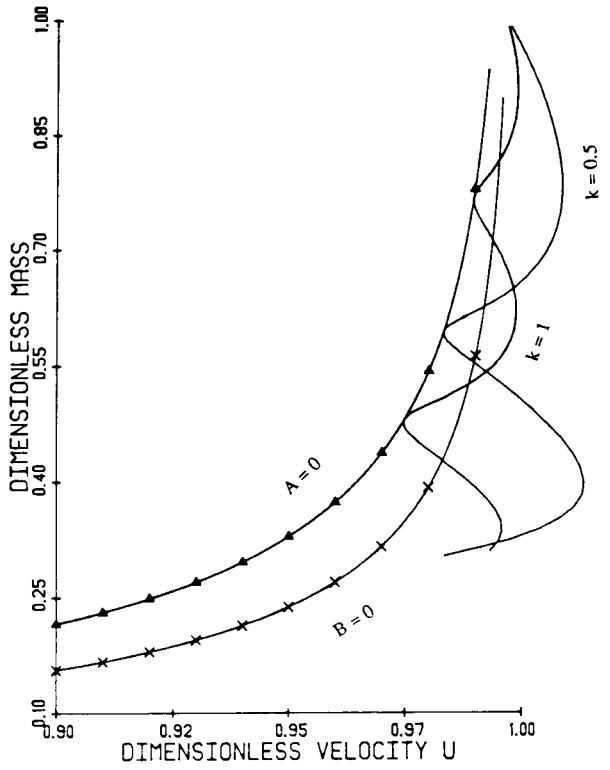

Fig. 4 The Dimensionless Velocity u vs. Mass μ History and Crossing Points (Z = 0.080640)

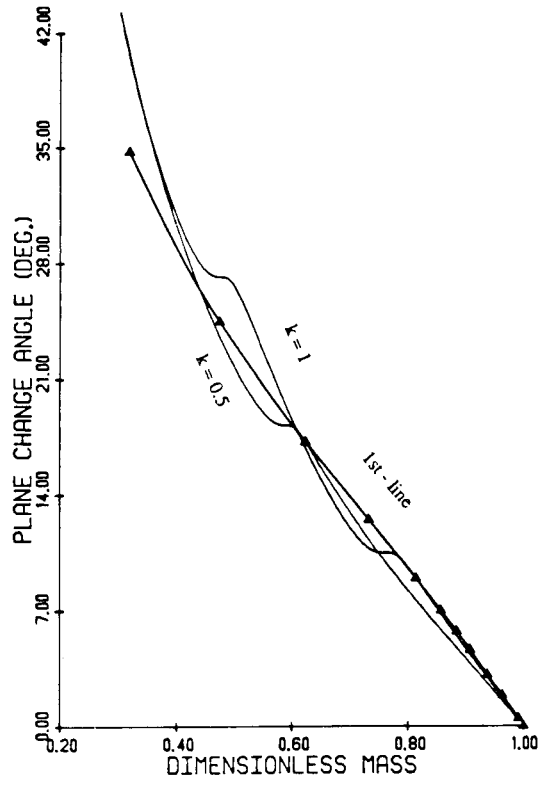

Fig. 5 The Variation of Plane Change i vs. Mass μ (Z=0.080640)

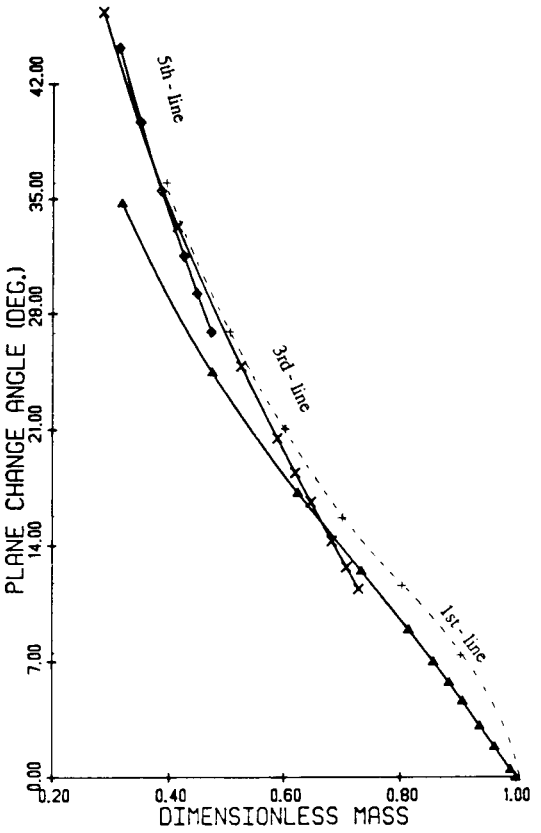

Fig. 6 The Optimal Plane Change Angle i (Z=0.080640)

When B = 0 , A is not necessarily zero. Hence, we deduce that when B = 0, we have

$$\frac{Z^2}{\mu^2} = \frac{1-u}{u^2}\left[(1+u) + (1-u)\frac{\sqrt{u}}{c} \right] \tag{54}$$

which is the same as Eq.(47). This relation between u and μ corresponds to the curve labelled " B=0 " in Fig. 4. Any pure sustaining-arc should start and end on the "B=0" curve. For a long trajectory (corresponding to small μ_f), it may touch the "A=0" curve a few times and cross the "B=0" curve a few times. For a short trajectory, however, it may not touch the "A=0" curve at all, i.e., there may be no bank reversals.

In order to determine the value of k corresponding to the globally maximizing controls, we must consider the achieved plane change, which is our measure of performance. Fig. 5 shows the relation between the plane change i and the residual mass ratio μ along the two trajectories k=1 and k=0.5. For a given k value, we find that each crossing of the B=0 curve in Fig. 4 corresponds to either a peak or a valley in the corresponding curve in Fig. 5. Specifically, the odd numbered crossing points in the sequence (counting in the direction of decreasing mass ratio), i.e. 1, 3, 5, etc., correspond to local maxima, while the even numbered crossing points in the sequence, i.e. 2, 4, 6, etc., correspond to local minima. When k is larger than 20, the first crossing point almost coincides with the initial point. For very large k, the trajectories are nearly the same. This is because the bank angle control, as given by Eq. (34), does not depend on k and the only term in the expression for the thrust control containing k

(refer to Eqs. (36)-(38)) is a homographic function of k and has the same asymptotic expression for large k.

Now, we examine Fig. 5 to find the global maximum. For a small amount of fuel consumption (i.e., a large μ_f), the first crossing point obviously corresponds to the optimum solution, but this is not necessarily true for a larger amount of fuel consumption. The curve labelled "1st-line" in Fig. 5 represents the pair (μ_f, i_f) at the first crossing point, as a continuous function of k. We see that the k=1 curve crosses the 1st-line, and moves above it, around μ_f = 0.62. This suggests that the third crossing point may correspond to a larger plane change after some μ_f.

By plotting the 1st-line, the 3rd-line (which corresponds to the 3rd crossing point), and the 5th-line (see Fig. 6), the optimal crossing point for each value of μ_f is clearly seen. The 3rd-line crosses the 1st-line around μ_f = 0.67. Thus, when μ_f is between 1 and 0.67, the first crossing point denotes the globally maximum solution; the corresponding k value uniquely defines the optimal controls. The 5th-line crosses the 3rd-line around μ_f = 0.32; so, when μ_f is between 0.67 and 0.32, the third crossing point denotes the optimal solution.

Fig. 6 is essentially the plot of the maximum plane change i_f versus the final mass ratio μ_f. The plot is continuous but its slope is discontinuous at the junction points of the different lines. This is because we have assumed that the optimal trajectory is a pure sustaining-arc, and consequently the final velocity, u_f, is determined from Eq.(50) and in general does not satisfy the prescribed end condition (11). If we require u_f to be the same value for each trajectory, then i_f, as a function of μ_f, will have a continuous first derivative. If the specified common value of u_f is higher than the value achieved on the pure sustaining-arc, for a particular trajectory, then a final boosting-arc is required. If the specified value of u_f is lower, then a final coasting-arc is required. The transversality condition, to be satisfied at the final time is still $B_f = 0$, but as given by Eq.(45), rather than by Eq.(49) which was derived for a sustaining-arc.

To illustrate the point made in the previous paragraph, we select a common value of u_f = 0.95. Then for each specified μ_f, we guess the value of k and integrate the equations for a pure sustaining-arc as before. When μ attains μ_f with $u > 0.95$, the switch is made to coasting flight, i.e., to $\tau = 0$, but now with the bank control X obtained from Eq.(28). At the final velocity u_f=0.95, the transversality condition (45) is checked. This procedure is repeated until the value of k that satisfies the transversality condition is found. Carrying out the computations, we find that the total plane change i_f is now higher as shown by the dashed line in Fig. 6; and there are no discontinuities in the slope.

Similarly, the initial velocity for the sustaining-arc does not in general satisfy the prescribed initial condition (10). So it follows that a boosting-arc or a coasting-arc would preceed the sustaining-arc.

We are now in a position to compare the sustaining-arc solution, in which the bank angle (or equivalently, the angle of attack) and the thrust are modulated, to the steady cruise solution, in which the angle of attack and the thrust are constant. We consider the same altitude as above, for which Z = 0.080640, and specify that μ_f = 0.6. The sustaining-arc solution gives a plane change of i_f = 19.7°; the highest lift coefficient required is about λ = 1.2. For the steady cruise case, the bank angle is given by the equilibrium condition (6); while, the thrust is set to cancel the drag. Solving the parametric optimization problem to obtain the optimal velocity and lift coefficient, we obtain the optimum values u = 0.998 and λ = 1.8. The bank angle increases from the initial value of 89.2° to the final value of 89.5°. The time of flight is shorter. The resulting plane change is i_f = 17.6°.

However, the comparison is not complete since the steady cruising velocity is slightly higher than both the initial velocity u_0 = 0.9968 and the final velocity u_f = 0.9912 for the sustaining-arc. These differences are adjusted by adding an initial coasting-arc to the sustaining-arc and prolonging the steady turn by a final coasting-arc. Consider the two equations for u and ψ in the new form

$$\frac{du}{ds} = -\frac{u Z (1+\lambda^2)}{E^* \mu}$$

$$\frac{d\psi}{ds} = \frac{Z\lambda}{\mu} \sin\sigma - \cos\psi \tan\phi \qquad (55)$$

Neglecting the small term in $\tan\phi$, we combine these equations to obtain

$$\frac{d\psi}{du} = -\frac{E^* \lambda \sin\sigma}{(1+\lambda^2) u} \qquad (56)$$

The most favorable turn is conducted with λ = 1 and σ = 90°. Then by integrating from u_1 to u_2, we have

$$\Delta i \approx \Delta\psi = \frac{E^*}{2} \log\frac{u_1}{u_2} \qquad (57)$$

According to this formula, for a turn from u=0.998 to u=0.9912, the sustaining-arc provides a plane change of i_f = 19.7° + 0.08° = 19.78°; while, the steady turn yields a plane change of i_f = 17.6° + 0.47° = 18.07°. Although the improvement in plane change capability, attainable through angle of attack and thrust modulation, is small for the altitude considered, it becomes more and more substantial as the altitude increases. above, increases as the altitude increases.

Next we consider a sustaining-arc at a higher altitude corresponding to Z = 0.010913. The initial velocity for the sustaining-arc is u_0 = 0.999940, almost circular. If h is the altitude difference with respect to the previous flight level Z_0 = 0.080640 taken as reference, and β is the inverse scale height for an exponential atmosphere, the new value of Z satisfies the equation

$$\beta h = \log(Z_0 / Z) = 2 \ .$$

Hence the new altitude is about 15 km higher. Since the atmospheric density is lower, we would expect a longer range trajectory, for a given amount of fuel consumption, in comparison to the lower altitude case considered above.

Fig. 7 shows that there is even less deviation from circular velocity than there was at the lower altitude, namely, 0.1% versus 3.0%. From the number of intersections with the A=0 line, it is clear that, for a given amount of fuel consumption, more revolutions are required at higher altitude to achieve the plane change, as expected. Fig. 8 shows that the optimal number of revolutions increases as the propellant mass, one is willing to expend, increases.

Representative plots of the optimal controls for the higher altitude case are shown in Figs. 9-11. The value of μ_f

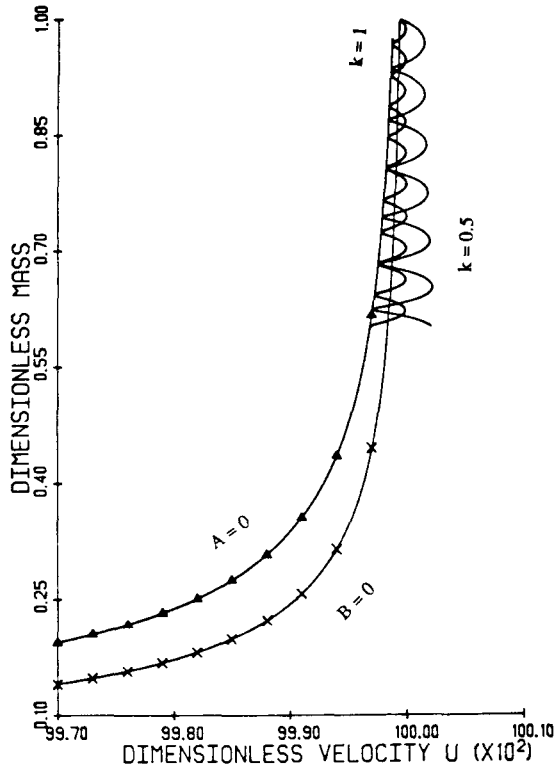

Fig. 7 The Dimensionless Velocity u vs. Mass μ History and Crossing Points (Z=0.010913)

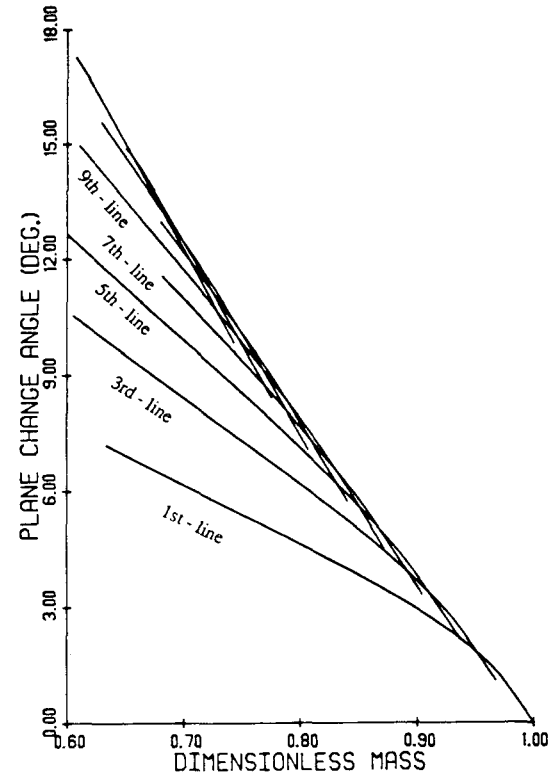

Fig. 8 The Optimal Plane Change Angle i (Z=0.010913)

is 0.6. For this case, it takes about five revolutions to achieve the optimal plane change. The optimal plane change is 17.8°, which is less than the 19.7° achievable in the lower altitude case, for the same fuel consumption. The optimal controls are nearly periodic. In Fig. 9, the latitude and the optimal bank angle are plotted against the longitude. The longitude is reset at $\theta = 0$ at the ascending node, $\phi = 0$, for a typical revolution. The increase in the absolute values of the maxima and minima of the latitude shows that the inclination is increasing. The optimal bank angle is nearly bang-bang. The optimal bank angle switches values at the apexes of the orbit. It is +90 degrees on the side containing the ascending node and -90 degrees on the side containing the descending node. A bank angle magnitude of 90 degrees assures that all the lift force is used for turning. The switching of the sign assures that the inclination continues to increase.

Fig. 10 shows the optimal normalized lift coefficient (which is directly related to angle of attack), along with the optimal bank angle, as functions of the longitude. It has been noted that the lift coefficient and the bank angle are related (see Eq. (6)). Previous work[2,6] has shown that, for a given heading angle change, the corresponding inclination change is maximized, if the heading change is made at a node. The behavior of the normalized lift coefficient is consistent with this finding. We see that the lift increases to its maximum at the nodes. The reason the lift is not always at its maximum is indicated in Fig. 11. Fig. 11 shows the normalized thrust magnitude as a function of the longitude. Since the lift vector is essentially always in the horizontal plane, the altitude is kept constant by flying at circular velocity. The control for maintaining nearly circular velocity is the thrust magnitude. Although maximum lift is good for turning, high lift means high drag. Consequently, the thrust magnitude is seen to peak in phase with the lift. The lift decreases to a minimum at the apexes of the orbit because heading changes lose their effectiveness in changing the inclination and because propellant can be saved. In contrast, the steady cruise turn, because the lift coefficient (angle of attack) and velocity are constrained to be constants, does not provide the freedom to compensate for the spatial non-uniformity in the effectiveness of out-of-plane forces to change the orbital plane; and consequently, the performance of the steady cruise turn deteriorates at high altitude.

As a final note, Fig. 11 shows that only a low thrust capability is required to fly the sustaining-arc at high altitude and accomplish a substantial plane change.

Conclusions

The problem of maximizing the orbital plane change during constant altitude flight has been formulated; and necessary conditions for the optimal trajectories and controls have been derived. The optimal trajectories are composed of boosting, coasting, and sustaining arcs -- the latter being a singular arc. Our interest in synergetic plane changing, with a constrained heating rate, led us to consider primarily the sustaining-arc. For the sustaining-arc, the optimal controls could be determined in feedback form, i.e., in terms of the states, except for a constant parameter. A combined numerical/graphical procedure was used to determine the globally maximizing solution from a family of extremals.

The primary physical conclusion of this paper is that, during constant altitude flight, the maximum plane change is not in general achieved by flying at a constant angle of attack, i.e., with a constant lift coefficient. The additional propellant consumption incurred by maintaining constant angle of attack grows as the range over which the flight takes place increases. Thus, the advantage of variable angle of attack flight increases as the flight altitude increases. For very high altitude flight,

which might be chosen to reduce the heating rate, the aerodynamic force is small, and it may take a substantial portion of a revolution, or even several revolutions, to effect the required plane change. In this case, the optimal angle of attack control becomes near-periodic. On the other hand, the velocity, although it has not been constrained to be constant, is nearly constant and approximately circular.

Acknowledgement--This work was supported in part by the Jet Propulsion Laboratory under contract No. 956416.

References

1. London, H. S., "Change of Satellite Orbit Plane by Aerodynamic Maneuvering," *Journal of the Aerospace Sciences*, Vol. 29, No. 3, March 1962, pp. 323-332.
2. Mease, K. D., Lee, J., and Vinh, N. X., "Orbital Changes During Hypersonic Aerocruise," *Journal of the Astronautical Sciences*, Vol. 36, No. 1/2, Jan.-June 1988.
3. Vinh, N. X., *Optimal Trajectories In Atmospheric Flight*, Elsevier, New York, 1981.
4. Dickmanns, E. D., "The Effect of Finite Thrust and Heating Constraints on the Synergetic Plane Change Maneuver for a Space Shuttle Orbiter-Class Vehicle," NASA TN D-7211, Oct. 1973.
5. Powell, R. W., Naftel, J. C., and Cunningham, M. J., "Performance Evaluation of an Entry Research Vehicle," Paper No. 86-0270, AIAA 24th Aerospace Sciences Meeting, Reno, Nevada, Jan. 1986.
6. Ikawa, H. and Rudiger, T. F., "Synergetic Maneuvering of Winged Spacecraft for Orbital Plane Change," *Journal of Spacecraft and Rockets*, Vol. 19, No. 6, Nov.-Dec. 1982, pp. 513-520.

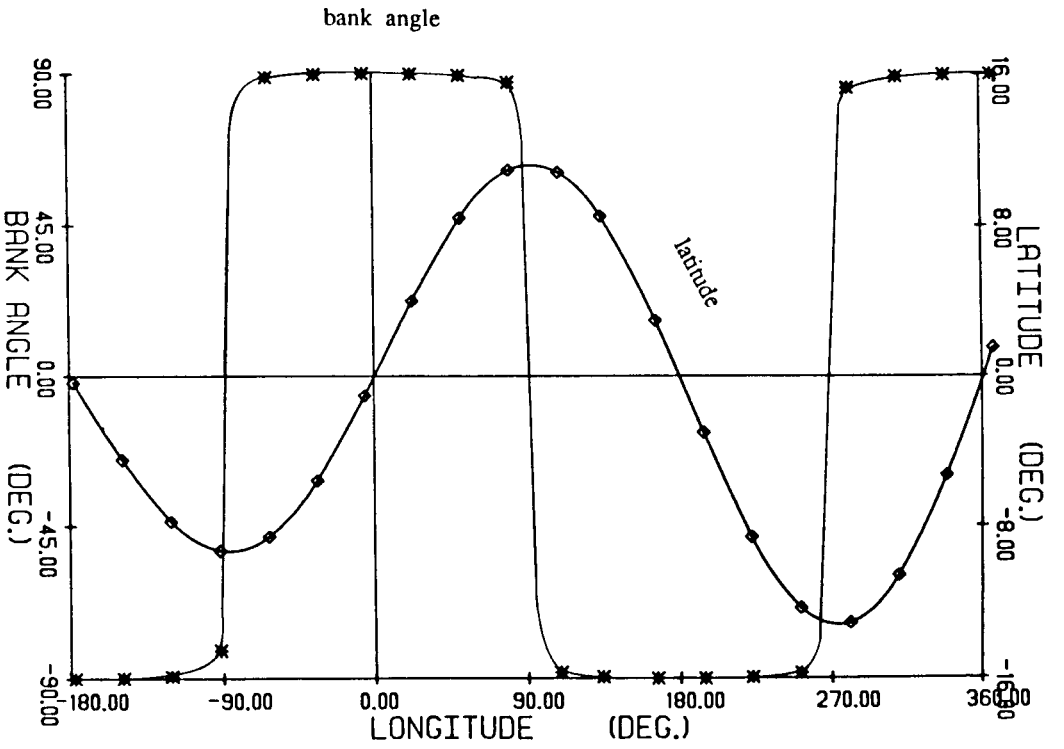

Fig. 9 Comparison between Bank Angle and Latitude along the Optimal Flight Path

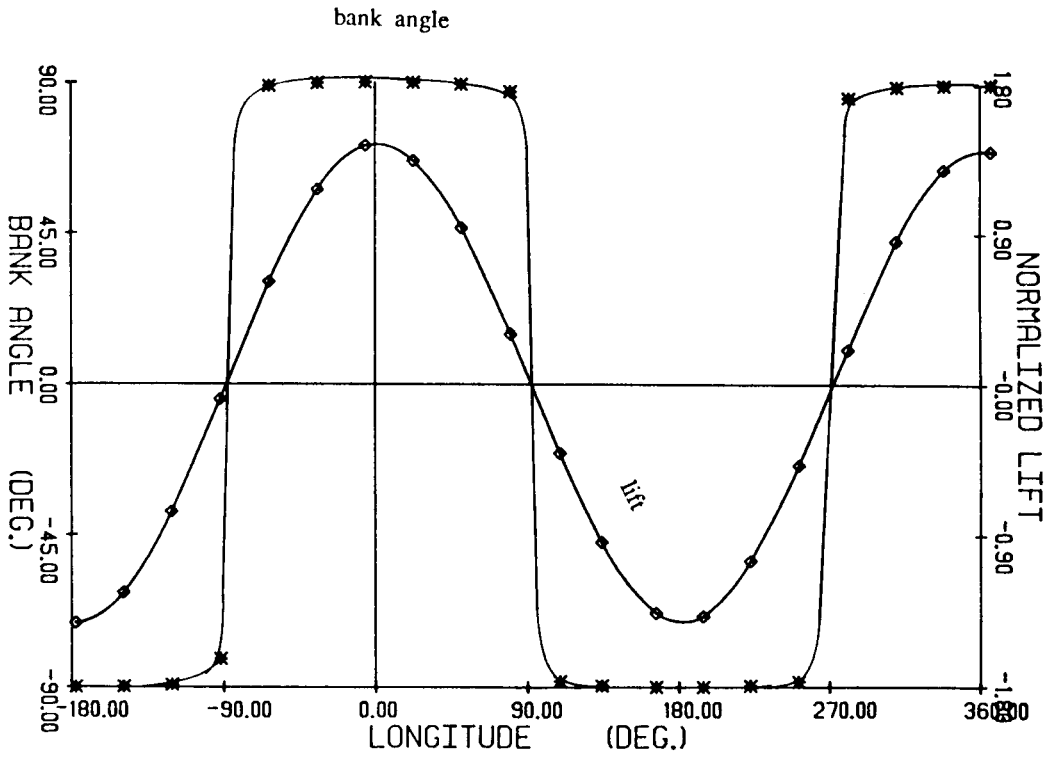

Fig. 10 Comparison between Bank Angle and Normalized Lift along the Optimal Flight Path

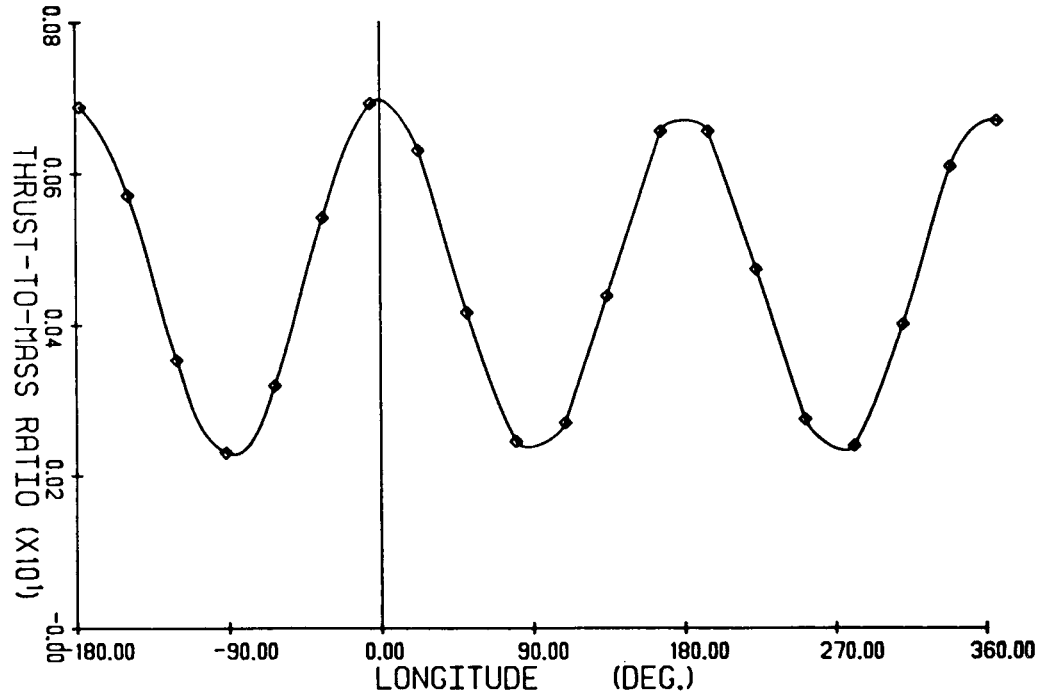

Fig. 11 Variation of Thrust along the Optimal Flight Path